Immobilization of Mn(I) and Ru(II) polypyridyl complexes on TiO2 nanoparticles for selective photoreduction of CO2 to formic acid

Long Le-Quang, Matthew Stanbury, Sylvie Chardon-Noblat, Jean-Marie Mouesca, Vincent Maurel, Jérome Chauvin

Journal Name

COMMUNICATION

Immobilization of Mn(I) and Ru(II) polypyridyl complexes on TiO_2 nanoparticles for selective photoreduction of CO_2 to formic acid

Received 00th January 20xx,
Accepted 00th January 20xx

DOI: 10.1039/x0xx00000x

www.rsc.org/

Long Le-Quang,[a,b] Matthew Stanbury,[a] Sylvie Chardon-Noblat,[a] Jean-Marie Mouesca,[b] Vincent Maurel[b] and Jérôme Chauvin*[a]

TiO_2 nanoparticles are successively functionalized with $[Mn(\kappa^2N^1,N^2\text{-ttpy})(CO)_3Br]$ as catalyst and $[Ru(bpy)_3]^{2+}$ as photosensitizer to yield $Ru^{II}/TiO_2/Mn^{I}$. Under continuous irradiation at 470 nm and in the presence of a sacrificial electron donor, this triad reduces CO_2 to HCOOH (TON_{max} = 27) with 100% selectivity.

Carbon dioxide (CO_2) is arguably one of the most notorious greenhouse gases that contribute to global warming[1] and rises in sea level.[2] In recent years, novel molecular catalysts able to reduce CO_2 into more value-added products have been extensively investigated to replace the prototypical $[Re(bpy)(CO)_3Cl]$ (bpy = 2,2'-bipyridine) catalyst.[3-5] Those based on earth-abundant elements such as Fe, Ni, Co, Cu and Mn are of particular interest,[6-8] not only for academics but also industrialists for potential upscaling.[9] Moreover, CO_2 conversion to produce useful compounds must be economically viable and photochemical reduction of CO_2, using renewable light energy source could be one of the solutions to solve the equation.

A general strategy to develop photoreduction system is to covalently link a photosensitizer with a molecular catalyst.[1,10,11] It, however, often requires challenging multi-step syntheses to obtain the desired supramolecules. An alternative approach, that combined also the advantage of heterogeneous catalysis,[12] consists to graft the photosensitizer and the catalyst onto the surface of nanoparticles (NPs) as they offer great surface area to accommodate the molecules.[7,13,14] This approach usually requires significantly less complicated syntheses than the supramolecular homogeneous approach and allows easy control of the surface occupancy and of the ratio between photosensitizer and catalyst. For instance, Neri *et al.*[15] grafted a $[Ru(bpy)_3]^{2+}$ photosensitizer (**Ru^{II}**) and a Ni(cyclam)$^{2+}$ (cyclam = 1,4,8,11-tetraazacyclotetradecane) catalyst on ZrO_2 NPs for photocatalytic CO_2 reduction. Under visible light and in the presence of ascorbic acid as a sacrificial electron donor, $Ru^{II}/ZrO_2/Ni^{II}$ system reduced CO_2 to a mix of CO and H_2. Meanwhile, the solution of homogeneous complexes **Ru^{II}** and Ni(cyclam)$^{2+}$ only produced traces of CO. The authors concluded that the proximal immobilization of the photosensitizer and the catalyst molecules on ZrO_2 surface enhanced the kinetics of photo-induced electron transfer reaction between **Ru^{II}*** and Ni(cyclam)$^{2+}$.

Semiconducting nanoparticles can also be used as both a substrate and an electron relay for the photo-induced electron transfer process between the photosensitizer and the catalyst. For instance, long lived charge separation state can be reach in nanostructured dye-sensitized TiO_2 photoelectrode thus facilitating multi-electron reduction reactions of CO_2.[16] For instance, Kang and co-workers[17,18] grafted an organic dye and $[Re(bpy)(CO)_3Cl]$ catalyst on TiO_2 NPs. Under visible light and in the presence of a sacrificial electron donor, the $Dye/TiO_2/Re^{I}$ system efficiently and selectively reduced CO_2 to CO with maximum turnover number (TON_{max}) surpassing 570 after 30 hours. In this work TiO_2 worked as an electron relay between the excited dye molecules and the Re(I) catalytic center.

As an alternative for rhenium complexes, manganese complexes have been extensively investigated in recent years. The prototype $[Mn(bpy)(CO)_3Br]$ is an efficient electrocatalyst[19] and was shown to work in association with **Ru^{II}** in a photocatalytic cycle[20] for the reduction of CO_2 to CO and HCOOH. Immobilization of this complex onto a (semi)conducting surface allowed for better product selectivity.[21-24] However, other Mn polypyridyl complexes than the bipyridines are still underexplored.[6,8] We recently reported the synthesis and characterization of a related complex $[Mn(\kappa^2N^1,N^2\text{-ttpy})(CO_3)X]^{n+}$ (ttpy = 4-tolyl-2,2':6'-2''-terpyridine) (X = Br and n = 0 or X = MeCN and n = 1).[25] Herein we present (i) the homogeneous electrocatalytic and photocatalytic reduction of CO_2 using $[Mn(\kappa^2N^1,N^2\text{-ttpy})(CO)_3Br]$ catalyst (**Mn^{I}**), and **Ru^{II}** photosensitizer and (ii) the immobilization of **Mn^{I}** and **Ru^{II}** on TiO_2 NPs ($Ru^{II}/TiO_2/Mn^{I}$, Scheme 1) for heterogenous photocatalytic CO_2 reduction.

[a] Department of Molecular Chemistry, UMR CNRS 5250, University of Grenoble-Alpes, CS 40700, 38058 Grenoble cedex 9, France. Email: jerome.chauvin@univ-grenoble-alpes.fr
[b] INAC, SyMMES, CEA Grenoble, F-38054 Grenoble, France. Email: vincent.maurel@cea.fr

Electronic Supplementary Information (ESI) available: See

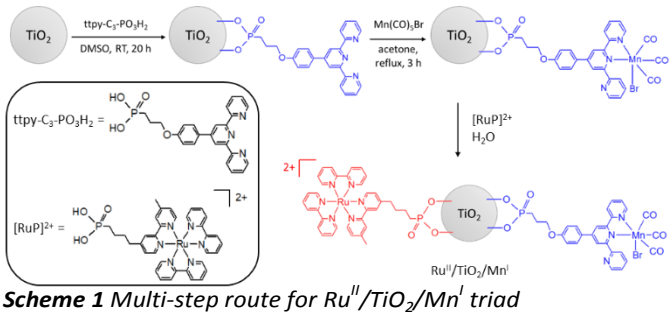

Scheme 1 *Multi-step route for $Ru^{II}/TiO_2/Mn^{I}$ triad*

The **Mn^{I}** complex was synthesized and characterized following a reported procedure[25] (see SI for more information).

Cyclic voltammograms (CVs) of **Mn^{I}** were recorded under argon in MeCN solution containing 0.1 M tetrabutylammonium hexafluorophosphate ($TBAPF_6$) (Figure 1, black line). The results are in accordance with the behavior of $[Mn(terpy)(CO)_3Br]$ (terpy = 2,2':6'-2''-terpyridine)[26] and the interpretation is based on relevant litterarure.[8,26,27] The CV is decoupled in figure S1. The first irreversible peak at E_{pc1} = -1.44 V is assigned to the $Mn^{+/0}$ one electron reduction process. This process leads to the leaving of Br^- and coordination of the free pyridyl of terpyridine to form a tridentate linkage between the ttpy ligand and Mn center (reaction S1-S3). This reduction event is associated to the release of a CO group and the formation of a Mn^0-Mn^0 dimer through metal-metal bonding (equation 1).

$$[Mn(\kappa^2\text{-ttpy})(CO)_3Br]+1e^- \rightarrow \tfrac{1}{2}\,[Mn^0(\kappa^2\text{-ttpy})(CO)_2]_2+CO+Br^- \quad (1)$$

On the reverse scan, the anodic peak at -0.89 V corresponds to the oxidation of the dimer (reaction S4). Further sweeping to more negative potentials leads to a second one-electron irreversible peak at E_{pc2} = -1.67 V that is ascribed to the reduction of the **Mn^0-Mn^0** dimer to form $[Mn^{-I}(ttpy)(CO)_2]^-$ species (reaction S5-S6). The peak at -1.67 V is associated with a small oxidation peak at -1.45 V corresponding to the oxidation of the newly formed $[Mn^{-I}(ttpy)(CO)_2]^-$ to regenerate the dimer species (reaction S7-S8).

Under CO_2 and in the presence of water (5% v/v) as a proton source, the CV of **Mn^{I}** shows significant enhancement in current magnitude on both reduction peaks at -1.44 V and -1.67 V (Figure 1a, red line). Without water, the CV shows negligible difference to the CV recorded under Ar. These results hence suggest that the electrocatalytic CO_2 reduction may occur at both potentials, as already observed for $[Mn(terpy)(CO)_3Br]$[26] and $[Mn(phen)(CO)_3Br]$[27] (phen = 1,10-phenanthroline).

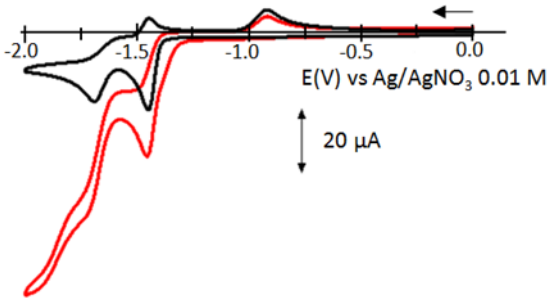

Figure 1 *CVs of **Mn^{I}** (1 mM) in MeCN + 0.1 M $TBAPF_6$ under Ar (black) and under CO_2 in the presence of 5% H_2O (red). v = 0.1 V s^{-1}.*

Controlled-potential electrolysis at -1.7 V produced CO as the only product (TON_{max} = 12, Faradaic efficiency (FE) = 100% after 4 h). This result shows remarkable improvement on catalytic activity and stability compared to $[Mn(\kappa^2\text{-terpy})(CO)_3Br]$ (TON_{max} (CO) = 4.1, FE = 129%)[26] where such an anomalously high FE could be a consequence of the decarbonylation of the complex as side reaction.

Photocatalytic CO_2 reduction experiments were carried out in DMF/TEOA mixed solution (TEOA: triethanolamine, C_{TEOA} = 1 M) in the presence of **Ru^{II}** as photosensitizer, **Mn^{I}** as catalyst and 1-benzyl-1,4-dihydronicotinamide (BNAH) as sacrificial electron donor. TEOA is added in the media as a base to suppress reverse reactionafter oxidation of BNAH.[28] Excitation wavelength was chosen at 470 ± 40 nm to selectively activate the photosensitizer and not the catalyst (Figure S1), as this catalyst can undergo photo-induced decarbonylation reaction.[29] After 16 h, the amounts of CO and H_2 in the gas phase and HCOOH in the liquid phase were measured by GC and HPLC, respectively (Table 1 entries 1-5, see SI for detail on the sample treatment and product quantification). Neither CO nor HCOOH was produced in the absence of **Mn^{I}** or light. We investigated various **Mn^{I}:Ru^{II}** ratios while keeping the **Ru^{II}** concentration unchanged so that light absorption by the photosensitizer remained the same in all the series. All the **Mn^{I}:Ru^{II}** ratios produced both CO and HCOOH while no H_2 was detected. Prolonging the irradiation time did not increase the product amounts. Table 1 shows that the decrease in the **Mn^{I}:Ru^{II}** ratio leads to a higher total TON. That may be due to two combined effects: a higher possibility for each **Mn^{I}** molecule being reduced by surrounding $[Ru(bpy)_3]^+$ molecules,

Table 1 *Results of the photocatalytic CO_2 reduction process. Solution: DMF/TEOA (1 M) and BNAH (0.1 M). Irradiation was achieved by using a Xe lamp ($3x10^{-4}$ W cm^{-2}, 5 cm apart), a UV-hot filter and a 470 ± 40 nm bandpass filter. Results were obtained after 16 h. TON uncertainties ± 2.*

Entry	Ratio of Mn^{I}:Ru^{IIa}	HCOOH n (µmol)	HCOOH TON_{max} [b]	CO n (µmol)	CO TON_{max} [b]	TON_{total} [c]
a) For homogeneous solution of Mn^{I} and Ru^{II} free complexes						
1	1:1	9.8	14	5.6	8	22
2	5:10	3.9	28	1.4	10	38
3	1:10	2.2	31	1.3	19	50
4	5:1	71.4	20	18.9	5	25
5	10:1	88.9	13	35.0	5	17
b) For $Ru^{II}/TiO_2/Mn^{I}$						
6	1:10	0.8	27	-	-	27

[a] Ru^{II} concentration is unchanged (0.14 mM)
[b] Turnover number (TON) *versus* Mn catalyst

produced by irradiation of **Ru^{II}** in presence of BNAH, and a protection of the **Mn^{I}** catalyst against photo-induced decarbonylation by an inner filter role of **Ru^{II}** which absorb more strongly visible light at 470 nm (ε (M^{-1} cm^{-1}) = 2300 for **Mn^{I}** and 8400 for **Ru^{II}**) (Figure S2). This property has already been observed for similar molecular photocatalytic systems.[11,15] In the series, the best **Mn^{I}:Ru^{II}** ratio is determined at 1:10 where the total TON reaches the highest value of 50.

We then prepared the triad **Ru^{II}/TiO$_2$/Mn^{I}** following a three-step procedure (Scheme 1, see SI for detail), in which phosphonic acid was chosen to anchor the complexes on anatase TiO_2 NPs.[30] It is noted that **Ru^{II}** was functionalized with only one phosphonic acid group in order to avoid it to be grafted on different TiO_2 NPs, which could lead to aggregation in colloidal solution. The ratio **Mn^{I}:Ru^{II}** = 1:10 was chosen following results in Table 1. After the immobilization of each complex, modified nanoparticles were separated by centrifugation and washed thoroughly with corresponding solvents. Maximum surface loading of **Mn^{I}** and **Ru^{II}** complexes was estimated at 14 µmol g^{-1} and 140 µmol g^{-1} ± 20 % respectively, by measuring the UV-visible absorbance of supernatant solutions after each centrifugation step. **Mn^{I}** complex was anchored first so that it can presumably be well distributed on TiO_2 surface and surrounded by **Ru^{II}** molecules. The presence of **Mn^{I}** on TiO_2 was confirmed by IR spectroscopy (Figure S3). The merging of two antisymmetric C≡O stretching bands after **Mn^{I}** has been grafted on TiO_2 is consistent with literature for Re[31] and Mn[21,22] triscarbonyl bipyridine complexes immobilized on TiO_2 NPs. The presence of **Ru^{II}** on TiO_2 was confirmed by UV-visible absorption and emission spectroscopies (Figure S4). The absorption maximum at around 450 nm of **Ru^{II}/TiO$_2$/Mn^{I}** is attributed to the singlet metal-to-ligand charge transfer (^{1}MLCT) absorption band of **Ru^{II}**.[32] In addition, its emission spectrum shows a maximum at 618 nm, which is characteristic of the ^{3}MLCT luminescence of $[Ru(bpy)_3]^{2+}$* state.[32] Meanwhile, **TiO$_2$/Mn^{I}** does not emit light in the 500-850 nm range under excitation at 450 nm.

Ru^{II}/TiO$_2$/Mn^{I} NPs were then tested in a photocatalytic CO_2 reduction experiment under the same conditions as described above for the mix of component complexes. The concentration of the NPs was kept at 0.4 g L^{-1} as higher concentrations lead to quick precipitation and light blocking. Surprisingly this system produced only HCOOH with a quantum yield of 0.17% and TON_{max} = 27 (Table 1 entry 6), while CO and H_2 were not detected. Control experiments using TiO_2 or **TiO$_2$/Ru^{II}** instead of **Ru^{II}/TiO$_2$/Mn^{I}** (amounts of TiO_2 and **Ru^{II}** were kept unchanged) produced no CO, H_2 or HCOOH, suggesting that HCOOH was formed only in the presence of **Mn^{I}** catalyst. In addition, when **TiO$_2$/Ru^{II}** NPs and free **Mn^{I}** complex were used instead of the triad, the results were comparable to the free complexes in homogeneous solution (i.e. production of both CO and HCOOH) (Table S1). These experiments suggest that the immobilization of the **Mn^{I}** catalyst on TiO_2 is related to the suppression of CO formation. The excellent yield and selectivity of HCOOH in this study surpass those of CO production from $[Re(bpy)(CO)_3Cl]$[33] and HCOOH production from $[Mn(bpy)(CO)_3Br]$[34] anchored on non-conducting support.

In order to elucidate the selectivity enhancement for HCOOH when **Mn^{I}** was anchored on TiO_2, we first used cyclic voltammetry to probe redox properties of immobilized **Mn^{I}**. A sample of **TiO$_2$/Mn^{I}** NPs powder was pressed inside the cavity of a platinum microelectrode and used as working electrode. Its CV recorded under Ar did not show a clear reduction signal upon cathodic scanning due to the population of electrons to the conduction band (CB) of TiO_2 from around -1.4 V *vs* $Ag/AgNO_3$ 0.01 M (Figure S5), which occurs at similar potential than the reduction of **Mn^{I}** (-1.44 V for free complex in solution). Therefore, we grafted **Mn^{I}** on a conductive Fluorine-doped Tin Oxide (FTO) electrode to investigate the electrochemical behavior of the immobilized **Mn^{I}** complex. FTO was chosen as phosphonic acid is a suitable anchoring group on this surface,[35] and it is rather redox-inactive up to -2 V. The CV of **FTO/Mn^{I}** electrode (Figure S6) shows a cathodic peak at E_{pc} = -1.43 V which is at the same potential as the first cathodic peak of the free complex in solution. However, on the reverse scan the associated anodic peak appears at a very different potential (E_{pa} = -1.16 V) than the peak recorded for the homogeneous complex in solution (-0.89 V), which has been assigned to the oxidation of the Mn^0-Mn^0 dimer formed after the first reduction step. Since **Mn^{I}** is immobilized, the formation of Mn^0-Mn^0 dimer should be prohibited. This assumption is supported by the lack of a second reduction process which is assigned to the reduction of the Mn^0-Mn^0 dimer in solution at -1.67 V. Scanning to potentials more negative than -2 V lead to the degradation of the FTO surface itself. Therefore, we conclude that the reduced form of immobilized complex is monomeric $[Mn^0(ttpy)(CO)_3]$ or $[Mn^0(ttpy)(CO)_2(MeCN)]$ and not the dimer observed for the complex in solution. The monomeric form of a related complex, $[Mn^0(bpy)(CO)_3Br]$, anchored on a metal-organic framework[36] or on TiO_2 particules[22] was proposed to be the intermediate to access 100% selectivity for HCOOH.

Previous works on the mixture of **Ru^{II}** and $[Mn(bpy)(CO)_3Br]$ in solution and using BNAH as sacrificial electron donor have shown that, under irradiation, **Ru^{II}** is first reductively quenched by BNAH to produce **Ru^{I}** and then **Ru^{I}** transfers an electron to the catalyst.[20] In the triad **Ru^{II}/TiO$_2$/Mn^{I}**, reduction of **Mn^{I}** may proceed via a similar process on surface between adjacent complexes, but more probably after population of the CB of TiO_2 from the **Ru^{II}*** excited state, since the injection of charge from **Ru^{II}*** is known to be very fast (k_{inj}> 10^{11} s^{-1}).[37] To understand whether the TiO_2 matrix participate to the electron transfer process and if the electrons injected in the CB of TiO_2 can reduced the **Mn^{I}** catalyst, we performed CO_2 reduction experiments using a mix of free **Mn^{I}**, BNAH and **SiO$_2$/Ru^{II}** or **TiO$_2$/Ru^{II}** NPs in DMF/TEOA mixed solution. Both systems contained the same concentration of Mn^{I} and BNAH in solution. They give rise to different results (table S1), with an enhancement of the production of HCOOH and CO with TiO_2 (TON_{total} = 44) instead of SiO_2 (TON_{total} = 12) as support for the **Ru^{II}** complex. We postulate then that the electron injected in the CB of TiO_2 from **Ru^{II}*** participate to the reduction of the **Mn^{I}**. The large surface of the TiO_2 NPs favours the reduction of the **Mn^{I}** complex in solution leading to an increase in the TON

compared to the SiO_2/Ru^{II} based system where the charge injection in the NPs is not possible and the reduction of Mn^{I} only occurs from specific site of Ru^{I} transient species on surface (energy diagrams in scheme S2 and S3 summarize the photoinduced electron transfer events). EPR spectroscopy was also performed on TiO_2/Ru^{II} and $Ru^{II}/TiO_2/Mn^{I}$ under irradiation with BNAH to confirm the charge injection and the presence of $BNAH^{+\bullet}$. For $Ru^{II}/TiO_2/Mn^{I}$, a lower signal is obtained for Ti3+ sites due to the electron transfer toward from the CB to the catalyst (see figure S7 and discussion underneath).

To sum up, Mn^{I} tolylterpyridine derivative appears as promising catalyst for the reduction of CO_2. When immobilized onto TiO_2 together with Ru^{II} as photosensitizer, the system efficiently and selectively reduces CO_2 to HCOOH with a quantum yield of 0.17% under visible irradiation. Cyclic voltammetry suggests that monomeric Mn^{0} complexes are the catalytically active sites in the $Ru^{II}/TiO_2/Mn^{I}$ hybride system whereas in a mixed solution of Ru^{II} and Mn^{I}, a Mn^{0}-Mn^{0} dimer is formed as a precatalyst. Heterogenization prevents the formation of dimers and achieves 100% selectivity toward HCOOH production.

Conflicts of interest

There are no conflicts to declare.

Acknowledgement.

The authors thank the LabEx ARCANE (ANR-11-LABX-0003-01) and O3H-EUR-GS (ANR-17-EURE-0003) for financial support.

References

1 C. D. Windle and R. N. Perutz, *Coord. Chem. Rev.*, 2012, **256**, 2562–2570.

2 R. M. DeConto and D. Pollard, *Nature*, 2016, **531**, 591–597.

3 J. Hawecker, J.-M. Lehn and R. Ziessel, *J. Chem. Soc. Chem. Commun.*, 1983, 536–538.

4 J. Hawecker, J.-M. Lehn and R. Ziessel, *J. Chem. Soc. Chem. Commun.*, 1984, 328–330.

5 Y. Kuramochi, O. Ishitani and H. Ishida, *Coord. Chem. Rev.*, 2018, **373**, 333-356.

6 N. Elgrishi, M. B. Chambers, X. Wang and M. Fontecave, *Chem. Soc. Rev.*, 2017, **46**, 761–796.

7 K. E. Dalle, J. Warnan, J. J. Leung, B. Reuillard, I. S. Karmel, E. Reisner, *Chem. Rev.*, 2019, **119**, 2752–2875

8 M. Stanbury, J.-D. Compain and S. Chardon-Noblat, *Coord. Chem. Rev.*, 2018, **361**, 120–137.

9 Y. Zheng, W. Zhang, Y. Li, J. Chen, B. Yu, J. Wang, L. Zhang and J. Zhang, *Nano Energy*, 2017, **40**, 512–539.

10 A. Sinopoli, N. T. La Porte, J. F. Martinez, M. R. Wasielewski, M. Sohail, *Coord.Chem. Rev.*, 2018, **365**, 60-74.

11 Y. Yamazaki, H. Takeda and O. Ishitani, *J. Photochem. Photobiol. C Photochem. Rev.*, 2015, **25**, 106–137.

12 K. Li, B. Peng and T. Peng, *ACS Catalysis*, 2016, **6**, 7485-7527.

13 Y. Sohn, W. Huang, F. Taghipour, *Appl. Surf. Sci.*, 2017, **396**, 1696-1711

14 L. Wang, W. Chen, D. Zhang, Y. Du, R. Amal, S. Qiao, J. Wu, Z. Yin, *Chem. Soc. Rev.*, 2019, doi:10.1039/c9cs00163h.

15 G. Neri, M. Forster, J. J. Walsh, C. M. Robertson, T. J. Whittles, P. Farras and A. J. Cowan, *Chem. Commun.*, 2016, **52**, 14200–14203.

16 E. Sundin and M. Abrahamsson, *Chem. Commun.*, 2018, **54**, 5289–5298.

17 E.-G. Ha, J.-A. Chang, S.-M. Byun, C. Pac, D.-M. Jang, J. Park and S. O. Kang, *Chem. Commun.*, 2014, **50**, 4462–4464.

18 D.-I. Won, J.-S. Lee, J.-M. Ji, W.-J. Jung, H.-J. Son, C. Pac and S. O. Kang, *J. Am. Chem. Soc.*, 2015, **137**, 13679–13690.

19 M. Bourrez, F. Molton, S. Chardon-Noblat and A. Deronzier, *Angew. Chemie, Int. Ed.*, 2011, **50**, 9903–9906.

20 H. Takeda, H. Koizumi, K. Okamoto and O. Ishitani, *Chem. Commun.*, 2014, **50**, 1491–1493.

21 T. E. Rosser, C. D. Windle and E. Reisner, *Angew. Chemie, Int. Ed.*, 2016, **55**, 7388–7392.

22 B. Reuillard, K. H. Ly, T. E. Rosser, M. F. Kuehnel, I. Zebger and E. Reisner, *J. Am. Chem. Soc.*, 2017, **139**, 14425–14435.

23 S.-J. Woo, S. Choi, S.Y. Kim, P. S. Kim, J. H. Jo, C. H. Kim, H.-J. Son, C. Pac, S. O. Kang, *ACS Catal.*, 2019, **9**, 2580-2593.

24 J. J. Walsh, M. Forster, C. L. Smith, G. Neri, R. J. Potter and A. J. Cowan, *Phys. Chem. Chem. Phys.*, 2018, **20**, 6811-6816.

25 J.-D. Compain, M. Stanbury, M. Trejo and S. Chardon-Noblat, *Eur. J. Inorg. Chem.*, 2015, 5757–5766.

26 C. W. Machan and C. P. Kubiak, *Dalt. Trans.*, 2016, **45**, 17179–17186.

27 J.-X. Zhang, C.-Y. Hu, W. Wang, H. Wang and Z.-Y. Bian, *Appl. Catal. A Gen.*, 2016, **522**, 145–151.

28 Y. Tamaki, T. Morimoto, K. Koike and O. Ishitani, *PNAS*, 2012, **109**, 15673-15678.

29 J.-D. Compain, M. Bourrez, M. Haukka, A. Deronzier and S. Chardon-Noblat, *Chem. Commun.*, 2014, **50**, 2539–2542.

30 R. Boissezon, J. Muller, V. Beaugeard, S. Monge and J.-J. Robin, *RSC Adv.*, 2014, **4**, 35690–35707.

31 C. D. Windle, E. Pastor, A. Reynal, A. C. Whitwood, Y. Vaynzof, J. R. Durrant, R. N. Perutz and E. Reisner, *Chem. Eur. J.*, 2015, **21**, 3746–3754.

32 A. Juris, V. Balzani, F. Barigelletti, S. Campagna, P. Belser and A. von Zelewsky, Coord. Chem. Rev., 1988, 84, 85–277.

33 C. Liu, K. D. Dubois, M. E. Louis, A. S. Vorushilov and G. Li, *ACS Catal.*, 2013, **3**, 655–662.

34 X. Wang, I. Thiel, A. Fedorov, C. Coperet, V. Mougel and M. Fontecave, *Chem. Sci.*, 2017, **8**, 8204–8213.

35 X. Marguerettaz and D. Fitzmaurice, *Langmuir*, 1997, **13**, 6769–6779.

36 H. Fei, M. D. Sampson, Y. Lee, C. P. Kubiak and S. M. Cohen, *Inorg. Chem.*, 2015, **54**, 6821–6828.

37 P. G. Giokas, S. A. Miller, K. Hanson, M. R. Norris, C. R. K. Glasson, J. J. Concepcion, S. E. Bettis, T. J. Meyer, A. M. Moran, J. Phys. Chem. C., 2013, 117, 812-824.